

## Intermittency analysis in heavy ion collisions: a review of the current status and challenges.

---

**Nikolaos Davis**<sup>a,\*</sup>

<sup>a</sup>*Institute of Nuclear Physics PAN,  
ul. Radzikowskiego 152, Kraków, Poland*

*E-mail:* [nikolaos.davis@ifj.edu.pl](mailto:nikolaos.davis@ifj.edu.pl)

The search for experimental signatures of the critical point (CP) of strongly interacting matter is one of the main objectives of numerous heavy ion collision experiments today. A promising category of CP observables are local fluctuations of the order parameter of the chiral phase transition, which are expected to be scale-invariant, following a universal power-law. An order parameter can be either the chiral  $\sigma$ -condensate, reconstructed through  $\pi^+\pi^-$  pairs, or the net baryon density  $n_B$ , and its proxy, the proton density.

Critical fluctuations of the order parameter can be probed through factorial moment intermittency analysis in transverse momentum space. Both dipion and proton intermittency analyses have been performed on NA49 SPS data, providing evidence of critical fluctuations in Si+Si collisions at 158A GeV/c [1, 2]. Probes of NA61/SHINE systems either show no intermittency (Be+Be, Pb+Pb), or are inconclusive (Ar+Sc); the analysis is complicated by the presence of large uncertainties, as well as difficulties in handling correlations [3]. We review the current status of intermittency analysis and discuss the challenges involved, such as particle identification and estimating the uncertainties of the intermittency index (power-law exponent  $\phi_2$ ). We propose solutions to these issues through novel statistical techniques and Monte Carlo simulations, presenting their advantages and drawbacks.

*Corfu Summer Institute 2021 "School and Workshops on Elementary Particle Physics and Gravity"  
29 August - 9 October 2021  
Corfu, Greece*

---

\*Speaker

## 1. Introduction

A key question in the study of QCD is to determine the structure of the QCD Phase Diagram as a function of temperature  $T$  and baryochemical potential  $\mu_B$  (equivalently: nuclear density,  $n_B$ ); that is, to determine the various states of strongly interacting matter, the Equations of State (EoS) that govern them, and the location, nature, and type of the phase transition boundaries that separate them. Fig. 1 shows a hypothetical sketch of the QCD Phase Diagram in  $(T - \mu_B)$ , where the phases of hadronic (nuclear) matter and quark-gluon plasma are separated by different types of phase transitions, namely a smooth cross-over at high  $T$  and low  $\mu_B$ , and a 1<sup>st</sup> order transition at low  $T$  and high  $\mu_B$ , ending on a critical point (CP), in the vicinity of which a 2<sup>nd</sup> order transition is expected to occur. Both the cross-over and the 1<sup>st</sup> order transition line are evidenced by Lattice QCD and effective models, respectively, and therefore there is ample evidence to support the existence of a critical point (CP) as an end point of the 1<sup>st</sup> order transition line.

A characteristic feature of a second order phase transition (expected to occur at the CP) is the divergence of the correlation length, leading to a scale-invariant system effectively described by a universality class. Of particular interest are local fluctuations of the order parameter of the QCD chiral phase transition, the chiral condensate  $\sigma(\mathbf{x}) = \langle \bar{q}(\mathbf{x})q(\mathbf{x}) \rangle$ . At finite baryochemical potential, the critical fluctuations of the chiral condensate are transferred to the net-baryon density [4]. For a critical system, we expect fluctuations of the order parameter to be self-similar [5], obeying power-laws with critical exponents determined by the 3D Ising universality class [6–8].

Candidates for the role of order parameter include the chiral  $\sigma$ -condensate as reconstructed through  $\pi^+\pi^-$  (dipion) pairs, as well as local fluctuations of the net baryon density  $n_B$ , and its proxy, the proton density in transverse momentum space. The choice of dipions offers the advantage of being the main decay channel of the  $\sigma$ -condensate, leading to an abundance of pions, and thus high-multiplicity events to analyse. However, this comes at the price of sifting through a large combinatorial background of unrelated  $\pi^+\pi^-$  pairs<sup>1</sup>. For that reason, intermittency analysis efforts were shifted to the study of net baryon density fluctuations, of which the net proton density is a proxy.

Such fluctuations correspond to a power-law scaling of the proton density-density correlation function, which can be detected in transverse momentum space within the framework of an intermittency analysis [8–11] of proton scaled factorial moments (SFMs). A detailed analysis can be found in Ref. [2], where we study various heavy nuclei collision datasets recorded in the NA49 experiment at maximum energy (158A GeV/c,  $\sqrt{s_{NN}} \approx 17$  GeV) of the SPS (CERN).

## 2. Methodology

### 2.1 The method of intermittency analysis

As mentioned in Section 1, critical fluctuations of the chiral phase transition order parameter follow a power-law form at the vicinity of the CP; specifically, for the idealized case of an infinite size system belonging to the 3D-Ising universality class, we obtain the following forms of density-

<sup>1</sup>A detailed dipion intermittency analysis of NA49 experimental data can be found in [1].

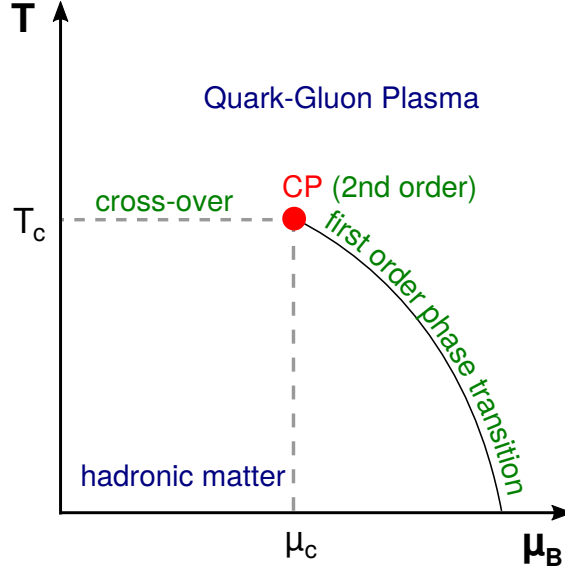


**Figure 1:** Hypothetical sketch of the phase diagram of strongly interacting matter with critical point, drawn as a function of baryochemical potential  $\mu_B$  and temperature  $T$ . A crossover transition is predicted at low  $\mu_B$  and high  $T$ ; whereas, a 1<sup>st</sup> order transition is predicted at low  $T$  and high  $\mu_B$ . A critical point (CP) is therefore hypothesized to exist as an end point of the 1<sup>st</sup> order transition line.

density correlations in momentum space, for the  $\sigma$ -condensate [6] and the net baryon density  $n_B$  [8], respectively:

$$\langle n_\sigma(\mathbf{k}) n_\sigma(\mathbf{k}') \rangle \sim |\mathbf{k} - \mathbf{k}'|^{-4/3} \quad (1a)$$

$$\langle n_B(\mathbf{k}) n_B(\mathbf{k}') \rangle \sim |\mathbf{k} - \mathbf{k}'|^{-5/3} \quad (1b)$$

where  $\mathbf{k} - \mathbf{k}'$  is the momentum transfer.

In order to probe a set of particle momenta for presence of power-law density-density correlations, we use the method of intermittency analysis of the Second Scaled Factorial Moments (SSFm)  $F_2(M)$ , pioneered by Białas and others [8–11] as a method to detect non-trivial dynamical fluctuations in high energy nuclear collisions. The method consists of partitioning an analysis window in transverse momentum space into a number of equal size bins (Fig.2), then examining how  $F_2(M)$  of particle transverse momenta scale with the number  $M^2$  of 2D bins:

$$F_2(M) \equiv \left\langle \frac{1}{M^2} \sum_{i=1}^{M^2} n_i(n_i - 1) \right\rangle / \left\langle \frac{1}{M^2} \sum_{i=1}^{M^2} n_i \right\rangle^2 \quad (2)$$

where  $n_i$  is the number of particles in the  $i$ -th bin, and  $\langle \dots \rangle$  denotes average over events.

For a pure critical system,  $F_2(M)$  is predicted to follow a power-law [6, 8]:

$$F_2(M) \sim M^{2 \cdot \phi_{2,cr}} \quad , \quad \phi_{2,cr}^{(\sigma)} = 2/3 \quad , \quad \phi_{2,cr}^{(p)} = 5/6 \quad (3)$$

where the exponent  $\phi_2$  is called the intermittency index.

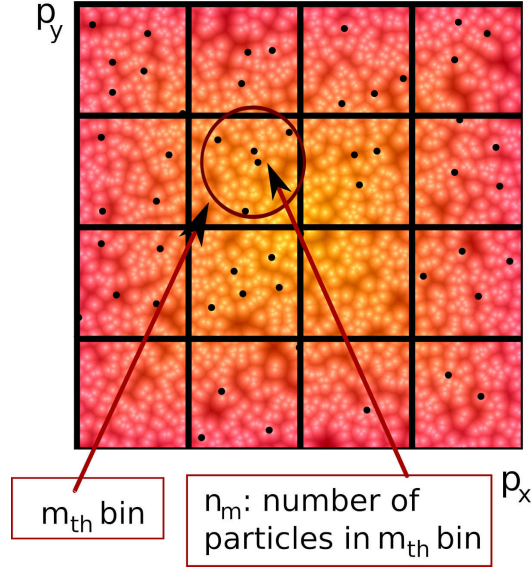


**Figure 2:** Counting particle pairs in a transverse momentum space partitioning of  $M \times M$  equal size bins. [Image by I. Sputowska]

For a noisy system, mixed event moments must be subtracted from the data moments in order to recover the critical component [2]. This is a non-trivial operation, starting with notionally partitioning all pairs in eq.(2) into critical/background pairs, plus a cross-term:

$$\langle n(n-1) \rangle = \underbrace{\langle n_c(n_c-1) \rangle}_{\text{critical}} + \underbrace{\langle n_b(n_b-1) \rangle}_{\text{background}} + 2\underbrace{\langle n_b n_c \rangle}_{\text{cross term}} \quad (4)$$

Rearranging (4), and normalizing to the mean particle multiplicity, we obtain:

$$\underbrace{\Delta F_2(M)}_{\text{correlator}} = \underbrace{F_2^{(d)}(M)}_{\text{data}} - \lambda(M)^2 \cdot \underbrace{F_2^{(b)}(M)}_{\text{background}} - 2 \cdot \underbrace{\lambda(M)}_{\text{ratio } \frac{\langle n \rangle_b}{\langle n \rangle_d}} \cdot (1 - \lambda(M)) f_{bc} \quad (5)$$

where  $\lambda(M) \equiv \langle n \rangle_b / \langle n \rangle_d$  is defined as the ratio of background to total (data) multiplicity in bins of size  $M$ .  $\lambda$  is in general a function of bin size, but in practice it converges to a constant value at the limit of  $M \rightarrow \infty$ , unless the 1-particle distribution is singular. The cross-term factor,  $f_{bc}$ , cannot in general be factored out into background and critical contributions, due to correlations between the two sets. However, Critical Monte Carlo [8] simulations show that the cross-term can be safely neglected [2] in two limit cases:

1. When  $\lambda(M) \sim 0$ , i.e. for an almost pure system, when background can altogether be ignored;
2. When  $\lambda(M) \lesssim 1$ , i.e. when the background is dominant, and background moments can be approximated by mixed event moments  $F_2^{(b)}(M) \sim F_2^{\text{mix}}(M)$ .

The latter (dominant background) has proved to be the case in virtually all experimental systems we have studied so far. We can thus simplify eq.(5), and define an effective correlator  $\Delta F_2(M)$  as simply the difference of data and mixed event moments:

$$\Delta F_2(M) = F_2^{(d)}(M) - F_2^{(m)}(M) \quad (6)$$

Intermittent behavior, if present, will then be revealed in  $\Delta F_2(M)$ ,

$$\Delta F_2(M) \sim (M^2)^{\varphi_2}, \quad M \gg 1 \quad (7)$$

and we obtain the predictions of eq.(3) for the intermittency index  $\phi_2$ , for the  $\sigma$ -condensate and proton density, respectively.

## 2.2 Handling of statistical and systematic uncertainties

SSFMs statistical errors are estimated via the bootstrap method [12, 13], which is a well-established statistical technique for obtaining unbiased error estimates of statistical quantities. In applying the bootstrap method to intermittency analysis, the original set  $S$  of events is first randomly sampled, with replacement, i.e., a number of events equal to that of the original set are selected uniformly at random; thus, a new bootstrap set  $S_B$  is created, in which some events are omitted and others repeated. By repeating this process, a large number of bootstrap samples  $S_{B_i}$ ,  $i = 1 \dots N_B$ ,  $N_B \gtrsim 1000$ , are created from the original set. Subsequently the quantity of interest, in particular the moments  $\Delta F_2(M)$ , are calculated for each bootstrap sample in the same manner as for the original; the resulting values can be used to obtain the bootstrap statistical distribution of  $\Delta F_2(M)$ , as well as its standard error, confidence intervals, or any other measure of variance desirable.

Bootstrap estimation of uncertainties has certain advantages over error propagation: it is straightforward to calculate, only requiring calculation of the original statistics (the SSFMs), in contrast to error propagation, which requires calculating higher moments [12]. It is relatively cheap computationally, as only the weights of each original event need to be calculated and stored in advance; the SSFMs of bootstrap samples can then be computed in one pass, along with those of the original. Finally, it allows us to naturally and effortlessly calculate the correlation matrix of  $\Delta F_2(M)$  between different bins  $M$ .

It must, however, be emphasized that the bootstrap cannot help us estimate or correct for the systematic uncertainties that may be present in the original sample. As verified by Monte Carlo simulations, as well as theoretical analysis, bootstrap estimates of the magnitude of variance and covariance of SSFMs can be trusted, but the centroids (average, median) estimated by bootstrap will certainly be biased towards the original sample. This is especially important to bear in mind when attempting to fit SSFMs with a power-law model, as in eq.(7):  $\Delta F_2(M)$  values for different  $M$  are not independent, as the same events are used to calculate all  $\Delta F_2(M)$ , and this invalidates a simple least-squares fit. We will address this issue, as well as methods to deal with it, in Section 5.

## 3. Results

### 3.1 NA49 dipion intermittency analysis

A pion intermittency analysis with the aim to detect QCD critical behavior was performed on data sets collected by the NA49 experiment [1, 14]. Analysis was conducted on a number of nuclear collisions of different sizes (p+p, C+C, Si+Si, Pb+Pb) at the maximum collision energy (158A GeV/c, corresponding to  $\sqrt{s_{NN}} \approx 17$  GeV) of the Super Proton Synchrotron (SPS), CERN.

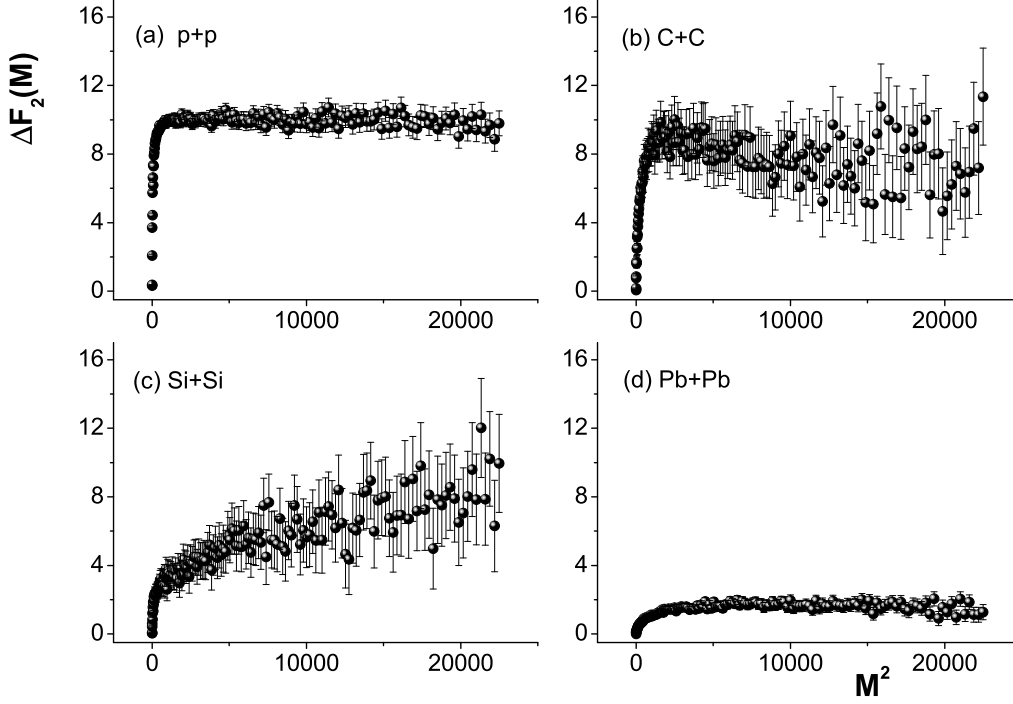


**Figure 3:** The correlator  $\Delta F_2(M)$  as a function of the number of 2-dimensional bins  $M^2$ , calculated for reconstructed dipions in transverse momentum space for (a) p+p, (b) C+C, (c) Si+Si, and (d) Pb+Pb NA49 experiment collisions at 158A GeV/c ( $\sqrt{s_{NN}} \approx 17$  GeV). Plot reproduced from [1].

In order to reconstruct the critical  $\sigma$  meson decay channel, the analysis was restricted to  $\pi^+\pi^-$  pairs with an invariant mass very close to the two-pion production threshold. A significant amount of combinatorial background had to be subtracted from  $F_2(M)$  in order to obtain the correlator  $\Delta F_2(M)$ , as described in Section 2.

Fig.3 shows the correlator  $\Delta F_2(M)$ , eq.(5), calculated after subtraction of background for dipion pairs in the invariant mass window chosen for the analysis, for (a) p + p, (b) C + C, (c) Si + Si, and (d) Pb + Pb NA49 experiment collisions at 158A GeV/c ( $\sqrt{s_{NN}} \approx 17$  GeV). No power-law scaling is observed for p+p, C+C and Pb+Pb collisions; in contrast, intermittent behavior approaching in size the prediction of critical QCD is observed for reconstructed dipions in Si+Si collisions, indicating a freeze-out state close to the critical point for the Si+Si system.

Fig.4 shows the intermittency index values  $\phi_2$  as a function of collision system size  $A$ , obtained by fitting the correlator  $\Delta F_2(M)$  of the analyzed systems with a power-law, eq.(7). Pb+Pb system is not included in the plot, as it did not meet the requirements for the invariant mass window reconstruction algorithm (see ref. [1]).

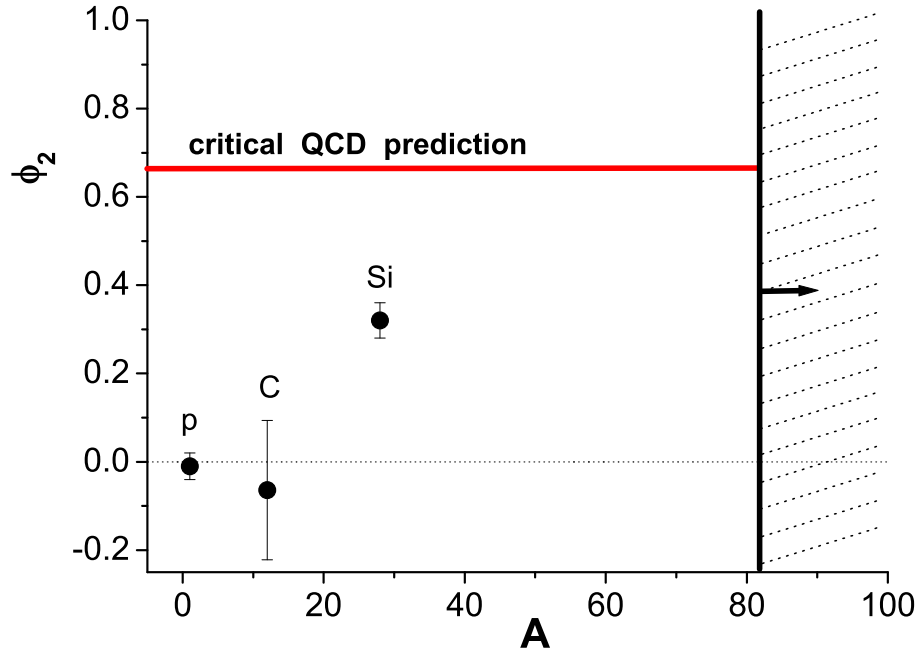


**Figure 4:** The fitted values of  $\phi_2$  for the A + A systems (A = p, C, Si) studied by NA49 as a function of system size A. The upper horizontal line presents the theoretically expected  $\phi_2$  value (2/3) for a system freezing out at the QCD critical point, while the lower horizontal line is at  $\phi_2 = 0$ . The shaded region indicates the A values for which the reconstruction algorithm is not conclusive. Shown error bars were obtained by analyzing subsamples. Plot reproduced from [1].

### 3.2 NA49 proton intermittency analysis

As mentioned in Section.1, pion intermittency analysis has the drawback of a large combinatorial background of non-critical  $\pi^+\pi^-$  pairs that need to be subtracted in order to reveal the critical dipion contribution originating from  $\sigma$  meson decays. For that reason, analysis efforts have been shifted to proton intermittency analysis, which probes the density-density correlations of the proton density, a proxy to the net-baryon density [4]. There are solid theoretical predictions for the expected  $\phi_2$  value of critical proton transverse momenta SSFMs [8]. This mode of analysis has the advantage of directly probing the proton density, and thus not requiring the subtraction of a combinatorial background. On the other hand, it has its own shortcomings: proton per event multiplicity is low in medium sized nuclei collisions (typically, of the order of  $\sim 2 - 5$  protons per event in systems such as C+C and Si+Si, and  $\sim 10$  in Pb+Pb). Therefore, an exceptionally large number of events (events statistics), and good proton identification are required in order for a proton intermittency analysis to be conclusive. At minimum of the order of  $\sim 100K$  events, and ideally more than  $\sim 1M$ , are needed in order to confidently establish a trend in  $\Delta F_2(M)$ ; proton purity (the percentage of actual protons in the candidate protons selected from the data) should ideally be in excess of 90%.

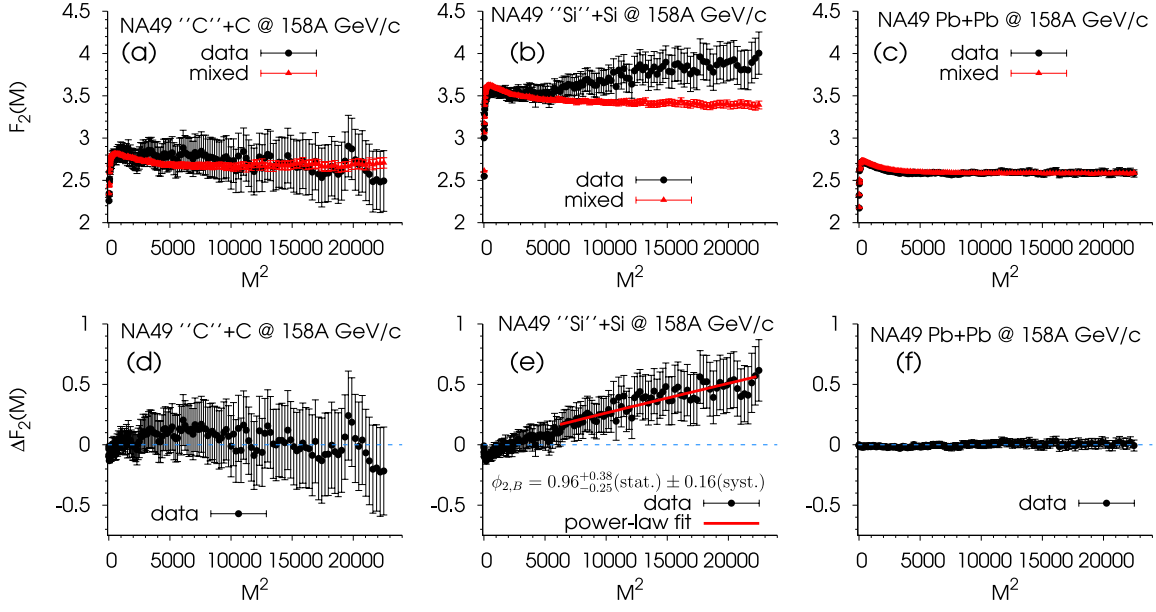


**Figure 5:** Proton SSFMs  $F_2(M)$  (top row) and the correlator  $\Delta F_2(M)$  (bottom row) for NA49 (a,d) C+C , (b,e) Si+Si , and (c,f) Pb+Pb most central (12%, 12%, 10%) collisions at 158A GeV/c ( $\sqrt{s_{NN}} \approx 17$  GeV) [2]. Error bars are calculated through the bootstrap method [12].

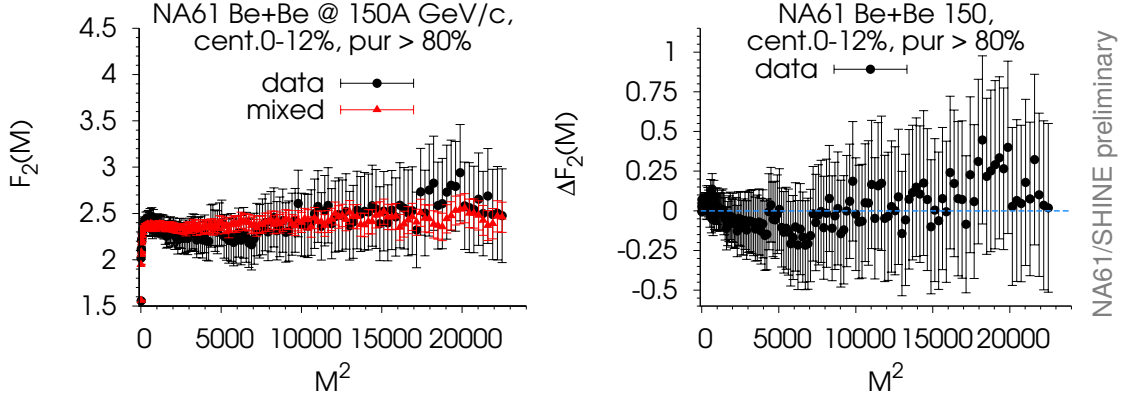
A proton intermittency analysis was performed on NA49 collision data sets [2], revisiting the same system sizes (C+C, Si+Si, Pb+Pb) and collision energy (158A GeV/c) as the aforementioned dipion analysis. For the purposes of the analysis, the most central (12% C+C, 12% Si+Si, 10% Pb+Pb) collisions were selected, as determined by the energy deposited in the Projectile Spectator Detector (PSD) downstream calorimeter [14]. The event statistics amounted to 148K events for C+C, 166K events for Si+Si, and 330K events for Pb+Pb. The standard event and track selection cuts of the NA49 experiment were applied. Proton identification used the measurements of particle energy loss  $dE/dx$  in the gas of the time projection chambers; tracks were accepted as candidate protons when the estimated probability of being a proton exceeded 80% for the C+C and Si+Si systems and 90% for Pb+Pb collisions. Finally, a window of analysis was selected in transverse momentum space ( $-1.5 \leq p_{x,y} \leq 1.5$  GeV/c), and candidate protons in the mid-rapidity region ( $|y_{CM}| \leq 0.75$ ) were projected in transverse space, where their SSFMs were calculated.

Fig.5 shows the SSFMs  $F_2(M)$  and the correlator  $\Delta F_2(M)$  for the analyzed NA49 systems. No intermittency effect is observed for the C+C (a,d) and Pb+Pb (c,f) systems; original data and mixed event moments overlap, and the correlator fluctuates around zero. In contrast, a significant intermittency effect is observed in the Si+Si system (b,e), as evidenced by the scaling of the corresponding  $\Delta F_2(M)$ , and in agreement with the dipion analysis result. The fitted power-law value for the intermittency index  $\phi_2$  is compatible with the theoretical prediction, eq.(3), however the statistical uncertainties are large.

### 3.3 NA61/SHINE proton intermittency analysis

Motivated by the positive, if ambiguous, NA49 proton intermittency Si+Si result, the search for the critical point through intermittency analysis has continued within the framework of the





**Figure 6:** Proton SSFMs  $F_2(M)$  (left) and the correlator  $\Delta F_2(M)$  (right) for NA61/SHINE Be+Be 12% most central collisions at 150A GeV/c ( $\sqrt{s_{NN}} \approx 16.8$  GeV) [16]. Error bars are calculated through the bootstrap method [12].

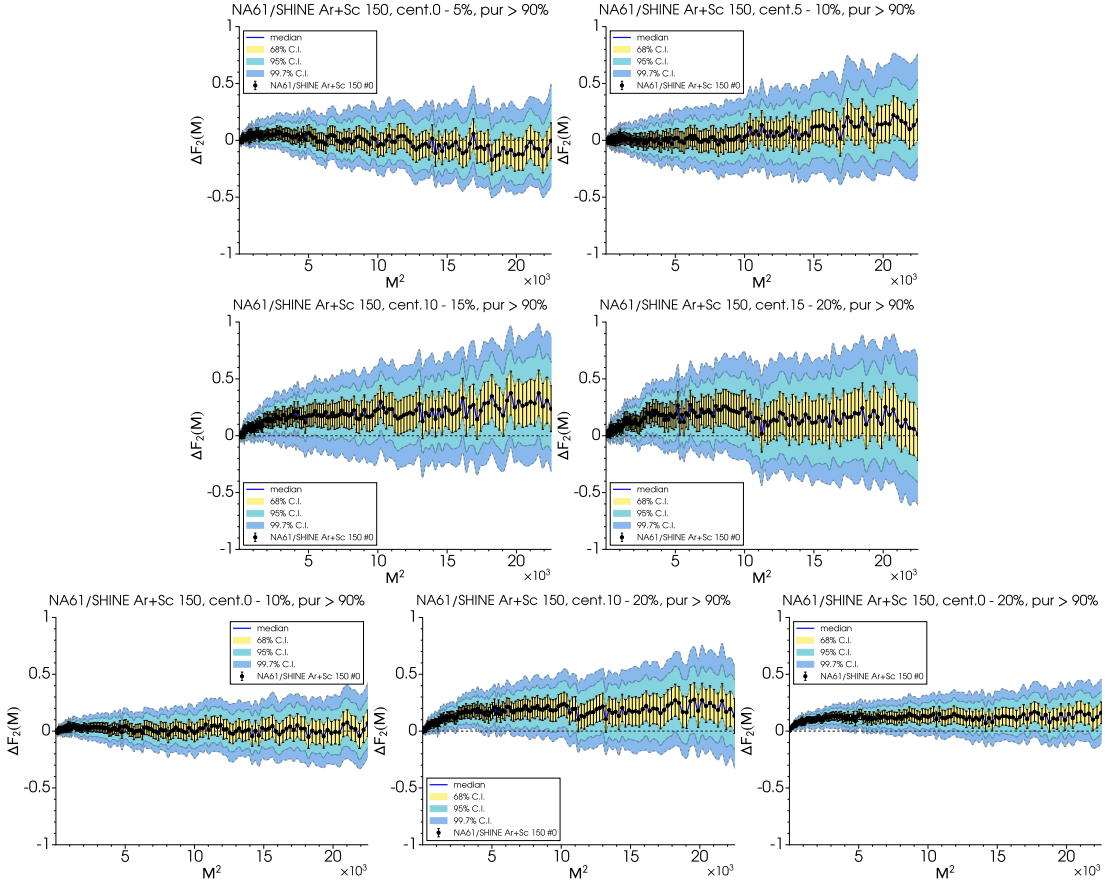
NA61/SHINE experiment [15]. NA61/SHINE is a fixed target, high-energy collision experiment at the SPS, CERN; it is the direct continuation of the NA49 experiment, and inherits most of its predecessor's detector setup as well as many of its experimental objectives, including the search for critical point signatures. NA61/SHINE has excellent capabilities for momentum vector reconstruction and particle identification in an extended regime of rapidity, as well as full coverage in the region of low transverse momenta, starting already at  $p_T = 0$ , and very good momentum resolution. The above features make NA61/SHINE one of the best choices of experiment for conducting an intermittency analysis scan.

The NA49 intermittency result suggests an experimental intermittency scan of medium-sized nuclei as the best candidates for the detection of the critical point. Preliminary analysis of a number of medium-sized NA61/SHINE systems (Be+Be, Ar+Sc at 150A GeV/c, corresponding to  $\sqrt{s_{NN}} = 16.8$  GeV) close in nuclear size to the NA49 Si+Si system was performed, to which end great effort was exerted in applying proper experimental cuts, the pre-selection of events and proton identification and selection.

Fig. 6 shows the SSFMs  $F_2(M)$  and the correlator  $\Delta F_2(M)$  for the analyzed Be+Be NA61/SHINE system [16]. No intermittency effect is observed, as  $F_2(M)$  of data and mixed events overlap, and therefore the correlator  $\Delta F_2(M)$  fluctuates around zero. It should be noted, however, that the average proton multiplicity per event in the Be+Be system was  $\sim 1.5$  in the mid-rapidity range, excluding events with a zero proton multiplicity; that is far too low for proton pair correlations to be firmly established, making it unlikely for an intermittency analysis to be able to detect a weak critical component, even if present, given the event statistics available ( $\sim 160$ K events).

Following Be+Be analysis, focus was shifted to studying the Ar+Sc system at 150A GeV/c, the closest in system size and collision energy to the NA49 Si+Si system. In this case, a full scan in collision centrality was performed, in the 0-20% most central range, in 5% and 10% intervals; the decision was due to experimental evidence, as well as theoretical understanding [3], that changes in collision peripherality influence the freeze-out conditions ( $\mu_B, T$ ) in a mild manner.

The first indication of intermittency in mid-central Ar+Sc collisions at 150A GeV/c was



NA61/SHINE preliminary

POS(CORFU2021)005

**Figure 7:** Proton SSFMs correlator  $\Delta F_2(M)$  for NA61/SHINE Ar+Sc 0-5%, 5-10% (*top row*), 10-15%, 15-20% (*middle row*), and 0-10%, 10-20%, 0-20% (*bottom row*) most central collisions at 150A GeV/c ( $\sqrt{s_{NN}} \approx 16.8$  GeV) [17]. Error bars are calculated through the bootstrap method [12]. Colored bands correspond to 1-(yellow), 2-(light blue), and 3- $\sigma$  (dark blue) confidence intervals, respectively.

presented at the CPOD2018 international conference [18]. In 2019, an extended event statistics set, approved by the NA61/SHINE Collaboration, was subjected to careful analysis. Event statistics were of the order of  $\sim 400K$  events per 10% centrality interval. Fig.7 shows the results of the NA61/SHINE Ar+Sc intermittency centrality scan, in the form of the correlator  $\Delta F_2(M)$  of proton SSFMs, for various collision centrality ranges. Centrality dependence is evident in the scaling of factorial moments, with the 0-5%, 5-10% (most central) collisions showing no evidence of intermittency, whereas the more peripheral collisions (10-15%, 15-20%) exhibit a weak intermittent effect. The dichotomy is most apparent in the 10% aggregated centrality intervals, with no signal in the 0-10% interval and a mild scaling effect in 10-20%, which even survives, weakened, in the overall 0-20% interval (total event statistics:  $\sim 800K$ ). Fig.7 also illustrates the magnitude and form of  $\Delta F_2(M)$  statistical uncertainties via confidence intervals (colored bands) corresponding roughly to 1,2 and 3- $\sigma$  variation around the experimental values (black points), as calculated via the statistical bootstrap.

It must be emphasized that such plots do not provide the full picture as to the  $\Delta F_2(M)$  variation and uncertainties, due to the presence of  $M$ -bin correlations: the errors of points with different

$M$  values, especially neighboring ones, are correlated, since the same set of events was used to calculate all the  $F_2(M)$ . This is the reason why confidence intervals for the intermittency index  $\phi_2$  cannot be properly obtained through simple power-law fitting, not even by fitting different bootstrap samples independently. The full  $\Delta F_2(M)$  covariance matrix has to be estimated and taken into account, which is subject to potential biases. Various approaches to the problem are being currently investigated, one of which, model weighting, will be presented in detail in the following sections.

#### 4. The Critical Monte Carlo simulation

The above review of experimental intermittency clearly shows that a better understanding is desirable of how SSFM scaling arises from criticality. The interplay of critical and non-critical protons, and the effect of a (dominant) background on the scaling and functional form of factorial moments, can be further investigated through model-building. Monte Carlo simulations provide a royal road towards such insights.

For this purpose, we use a modified version of the Critical Monte-Carlo (CMC) event generator [3, 6, 8] suited for simulating protons in transverse momentum space; simulated protons are produced through a truncated Lévy walk process to exhibit density-density correlations mimicking those originating from a fireball freezing out at the QCD critical point. The power-law exponent is chosen to describe correlations characterizing a critical system in the 3d-Ising universality class; associated intermittency index has the value  $\phi_2 = 5/6$ , corresponding to a fractal mass dimension of  $d_F = 1/3$  for the 2-dimensional Lévy walk. Furthermore, the algorithm can be parametrized to produce an exponential average per event proton  $p_T$  distribution for the random walk cluster centers, and a Poissonian per-event proton multiplicity distribution, the values of which can be plugged in; finally, truncated Lévy walk bounds can be fine-tuned in order to produce critical density-density correlations within the desired scales. A number of uncorrelated proton momenta drawn from a one-particle  $p_T$  distribution are interspersed among the critical protons at an adjustable percentage. These simulate the effect of non-critical background contamination on the critical signal, with the desired background level  $\lambda$ , eq.(5).

Fig.8 shows a family of CMC+background SSFMs, for simulated events corresponding to the characteristics of NA61/SHINE Be+Be (*left*) and Ar+Sc (*right*) systems at 150A GeV/c. In both cases, a number of events equal to the corresponding experimental statistics available were simulated, with the experimental  $p_T$  and proton multiplicity distributions replicated for the simulated events. Mixed events were also constructed from CMC events, and their SSFMs subtracted from the original moments to calculate  $\Delta F_2(M)$ . Comparing pure CMC moments (open triangles) to those of CMC + dominant background (filled triangles), we observe that  $\Delta F_2(M)$  retains the critical behaviour (scaling) of pure CMC, even though the moments differ by orders of magnitude in absolute value. For Be+Be, scaling persists almost up to a level of 99.7% of background (0.3% critical component), at which point  $\Delta F_2(M)$  of noisy CMC are comparable in size to the NA61/SHINE Be+Be moments (black points). Based on this result, we conclude that  $\sim 0.3\%$  is an upper limit for the percentage of critical protons in the NA61/SHINE Be+Be system – however, by the point  $\Delta F_2(M)$  of CMC and NA61/SHINE data have become comparable, intermittent behavior has almost completely deteriorated, which is compatible with the absence of intermittency in NA61/SHINE Be+Be.

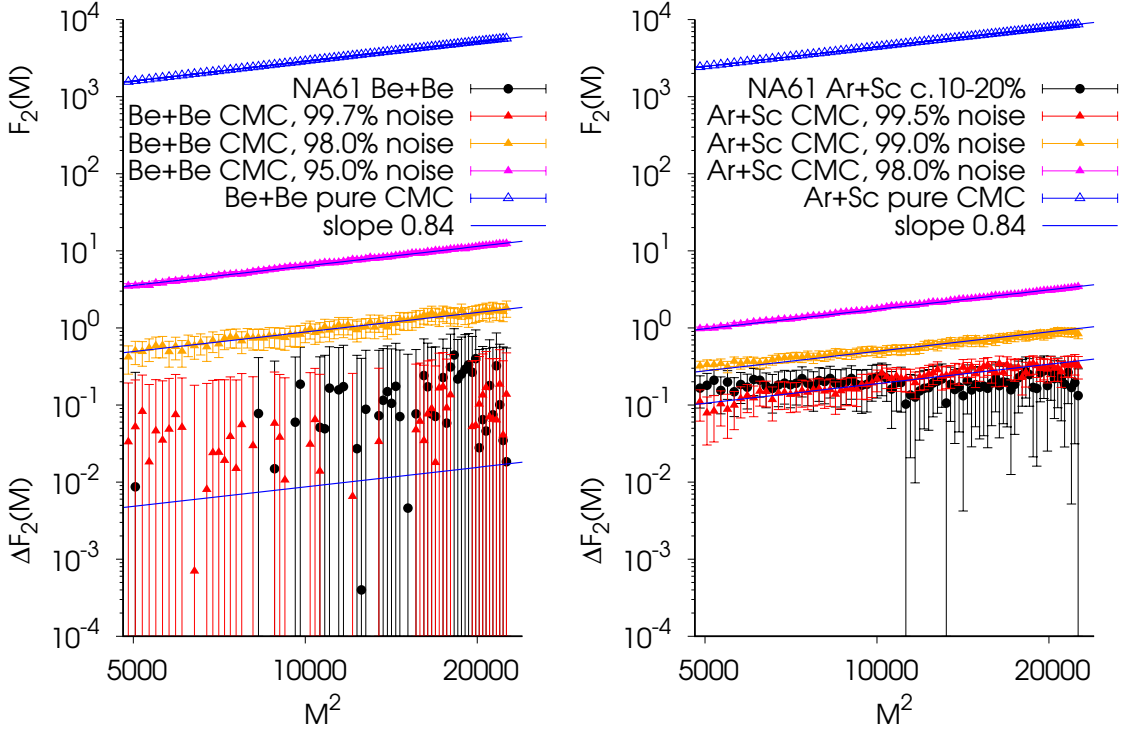


**Figure 8:** Comparison of Critical Monte Carlo (CMC) simulated SSFMs with NA61/SHINE experimental SSFMs, for different levels of non-critical proton background. (*left*) Simulation of a Be+Be-like system by a pure CMC (open triangles), as well as CMC+background for different background levels (filled triangles) [16]. Black points and error bars correspond to the NA61/SHINE experimental Be+Be  $\Delta F_2(M)$  values. (*right*) CMC simulation of an Ar+Sc-like system; interpretation of points & markers as in the left plot.

On the other hand, in the Ar+Sc 10-20% most central system simulation (*right*), we see that we retain a weakened, yet still recognizable power-law behavior down to the level of 0.5% critical component (99.5% background). Indeed, we have seen that there is a non-trivial scaling effect for Ar+Sc 10-20% (Fig.7, bottom center). We therefore conclude that  $\sim 0.5\%$  is an upper limit for the percentage of critical protons in the NA61/SHINE Ar+Sc system.

Critical Monte Carlo simulations give us an intuitive illustration of the way a critical effect is diluted in experimental data, and of the limitations in detecting critical scaling in systems with a dominant background component. Additionally, they provide an empirical justification for replacing the full correlator  $\Delta F_2(M)$  expression, eq.(5) with the “dominant background” approximation, eq.(6). Still, there is room for many significant improvements in the Monte Carlo. For instance, Lévy walk algorithm can be made more flexible, in order to allow us to simulate other values of  $\phi_2$  beyond the critical 5/6; also, CMC can be augmented with “afterburners” that simulate detector effects, such as quality and acceptance cuts, for better comparison with experimental data.

## 5. Challenges in intermittency analysis, and possible solutions

In performing intermittency analysis, in the form it is traditionally pursued, one faces a number of practical and methodological challenges that need to be dealt with in order to obtain statistically significant results. We list the most important among them below:

1. Particle species, especially protons, cannot be perfectly identified experimentally; candidates will always contain a small percentage of impurities. In the case of protons, the main contamination comes from  $K^+$  tracks misidentified as protons. In NA61/SHINE [15], we identify particles through their energy loss  $dE/dx$  in the Time Projection Chambers (TPCs), as a function of their momentum. Therefore, good particle identification requires quality decomposition of the total  $dE/dx$  spectra of tracks into a sum of gaussians of all particle species (p, K,  $\pi$ , e) in selected momentum space slices. Ideally, we accept candidate protons if they have an estimated probability of  $> 90\%$  of being a proton; however, there is a delicate balance between achieving a high enough proton purity, and keeping the total multiplicity of accepted protons large enough for the demands of an intermittency analysis.
2. Experimental momentum resolution sets a limit to how small a bin size (large  $M$ ) we can probe. Empirically, we have settled for a maximum of  $M = 150$  one-dimensional bins, which corresponds to a  $\Delta p_T$  of 20 MeV/c. Experimental momentum resolution is of the order of  $\sim 5$  MeV/c, well below our minimum bin size.
3. A finite (small) number of usable events is available for analysis; the “infinite statistics” behaviour of  $\Delta F_2(M)$  must be extracted from these. The best way to guard against finite statistics artifacts is to investigate as many CMC simulated data sets as possible, with an event statistics comparable to that of the experimental data.
4. Proton multiplicity for medium-sized systems is low (typically  $\sim 2 - 3$  protons per event, in the window of analysis) – and the demand for high proton purity lowers it still more. There is really no satisfactory solution to this issue, other than trying to increase event statistics. Failing that, we must turn to Monte Carlo simulation to gain insight about the statistical significance of our experimental data.
5.  $M$ -bins are correlated due to the fact that the same events are used to calculate all  $F_2(M)$ . This biases the fit algorithm for the intermittency index  $\phi_2$ , and makes confidence interval estimation hard.

The method of the statistical bootstrap (see Section 2.2) can help us up to a point to resolve issues #3-5, in providing unbiased estimators for the magnitude of statistical uncertainties of SSFMs. As mentioned, however, it is not sufficient for taking into account  $M$ -bin correlations and systematic errors in SSFMs. Replication of events means bootstrap sets are not independent of the original: magnitude of variance and covariance estimates can be trusted, but central values will be biased to the original sample. Correlated fits for obtaining  $\phi_2$  can be performed, using  $M$ -correlation matrix estimated via the bootstrap; however, these are known to be unstable: [19, 20]. Fig. 9 shows the results of a correlated (*left*) vs an uncorrelated (*right*) fit for the NA61/SHINE Ar+Sc 10-20%

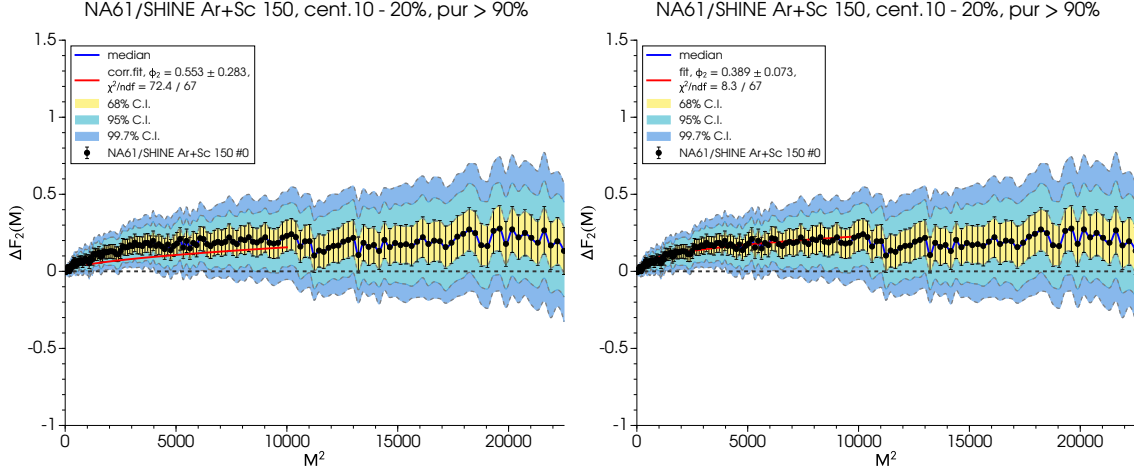


**Figure 9:** Correlated (*left*) and uncorrelated fit (*right*) for the NA61/SHINE Ar+Sc 10-20% most central system at 150A GeV/c.

most central system at 150A GeV/c. The correlated best fit line unintuitively passes below all experimental points, in contrast to the uncorrelated fit, which passes through them; the two methods also give considerably different values for  $\phi_2$  and  $\chi^2$  of fit.

The proposed solution to the problem of  $M$ -bin correlation is to avoid fitting for  $\phi_2$  altogether; rather, one should attempt to build a large number of Monte Carlo models, corresponding to different values of power-law scaling and critical component level, then weigh (test) these models against the experimental data. Thus, one can obtain probability distributions and confidence intervals for the physical quantities of interest that are incorporated in the model.

The AMIAS algorithm (Athens Model-Independent Analysis Scheme) [21, 22] can be used to extract model-independent parameter distributions such as the intermittency index  $\phi_2$  from sets of data. It works by sampling the (generally multi-dimensional) parameter space at random, then weighting selected models by goodness-of-fit function ( $e^{-\chi^2/2}$ ) to the dataset. Fig.10 shows the  $\phi_2$  distributions extracted by AMIAS from the NA61/SHINE Ar+Sc data sets at 150A GeV/c, for various centrality ranges. A simple power-law model was used as input to AMIAS:

$$\Delta F_2(M; a_0, \phi_2) = 10^{a_0} \left( \frac{M^2}{10^4} \right)^{\phi_2} \quad (8)$$

with model parameters  $a_0, \phi_2$ . The  $\phi_2$  distributions obtained provide us with a plausible range of intermittency index values that are compatible with the trends of the experimental SSFMs.

We can evaluate the performance of AMIAS by running it on simulated CMC datasets [3]. Fig.11 (*left*) shows  $\Delta F_2(M)$  values distribution for 400 independent CMC data samples of 400K events each; the simulated events (color bands) have been adjusted to fit the characteristics of the NA61/SHINE Ar+Sc dataset at 150A GeV/c, including the estimated critical component level. We notice that the 1<sup>st</sup> CMC set (black points) is typical among the simulated sets, wrt its deviation from the median trend. Fig.11 (*right*) shows the power-law model, eq.(8), parameter distributions ( $a_0, \phi_2$ ), and the corresponding weights ( $\chi^2$  values) obtained by AMIAS, by comparing the aggregated CMC sets to several million randomly chosen power-law models. We notice that AMIAS manages to

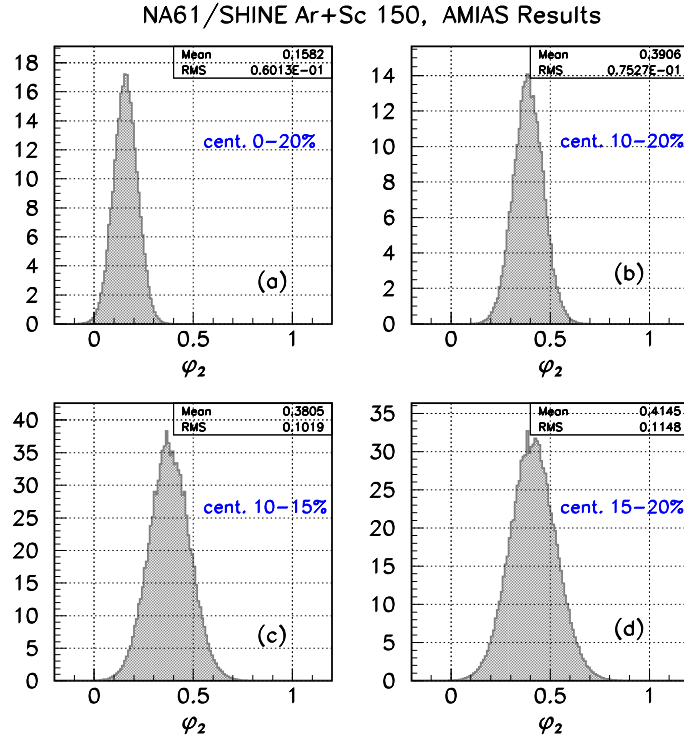


**Figure 10:**  $\phi_2$  distributions extracted by AMIAS from the NA61/SHINE Ar+Sc data sets for (a) 0-20%, (b) 10-20%, (c) 10-15%, and (d) 15-20% most central collisions at 150A GeV/c [3]. A simple power-law model, eq.(8), was used as input to AMIAS.

extract the plugged-in critical value of  $\phi_2$ , within errors, with excellent approximation ( $\phi_{2, \text{AMIAS}} = 0.83 \pm 0.06$ )

Finally, we must consider the statistical significance of the intermittency signal obtained for NA61/SHINE Ar+Sc. We can estimate it by comparing our experimental SSFMs to that of random, uncorrelated protons following the same 1-particle transverse momentum distribution. Fig.12 (left) shows  $\Delta F_2(M)$  values distribution for 1000 bootstrap samples of NA61/SHINE Ar+Sc data; these are compared to 400 independently produced samples of random background protons (right). We notice that, although random proton fluctuations can occasionally imitate an effect of comparable magnitude to the experimental data, this only happens roughly for  $\sim 5 - 15\%$  of the samples. At the same time,  $\sim 85 - 95\%$  of NA61/SHINE Ar+Sc bootstrap samples are above the zero line in  $\Delta F_2(M)$ . We therefore tentatively assign a  $\sim 5 - 15\%$  chance of random background producing a spurious effect, which is a small but non-negligible probability. It must be noted that this is still not a completely satisfactory statistical significance analysis: much more can be gained by systematically comparing experimental data to Monte Carlo models with various critical components, and taking into account  $M$ -bin correlations. This is possible with AMIAS coupled to the CMC model, and is currently work in progress.

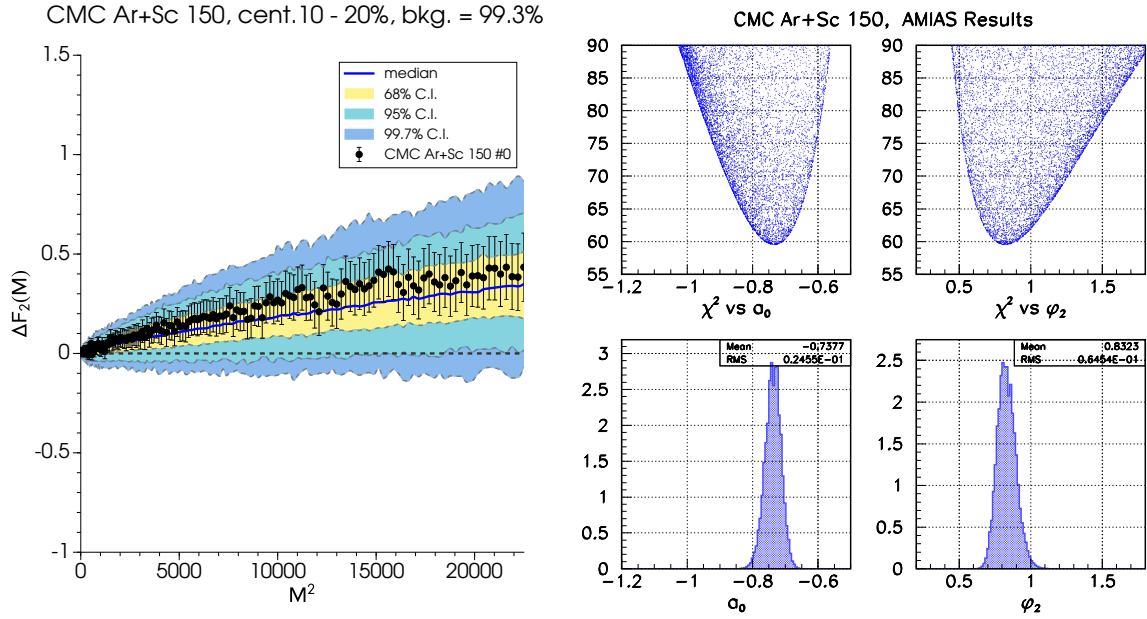


**Figure 11:** (left)  $\Delta F_2(M)$  values distribution for 400 independent CMC data samples (400K events each), with the characteristics of NA61/SHINE Ar+Sc at 150A GeV/c; the 1<sup>st</sup> CMC sample is shown as black points with error bars. (right) Power-law model, eq.(8), parameter distributions ( $a_0$ ,  $\phi_2$ ), and the corresponding weights ( $\chi^2$  values) obtained by AMIAS CMC/power-law model comparison. AMIAS predicts a  $\phi_2 = 0.83 \pm 0.06$  for the intermittency index, equal to the plugged-in critical value, within errors. Figures reproduced from [3]

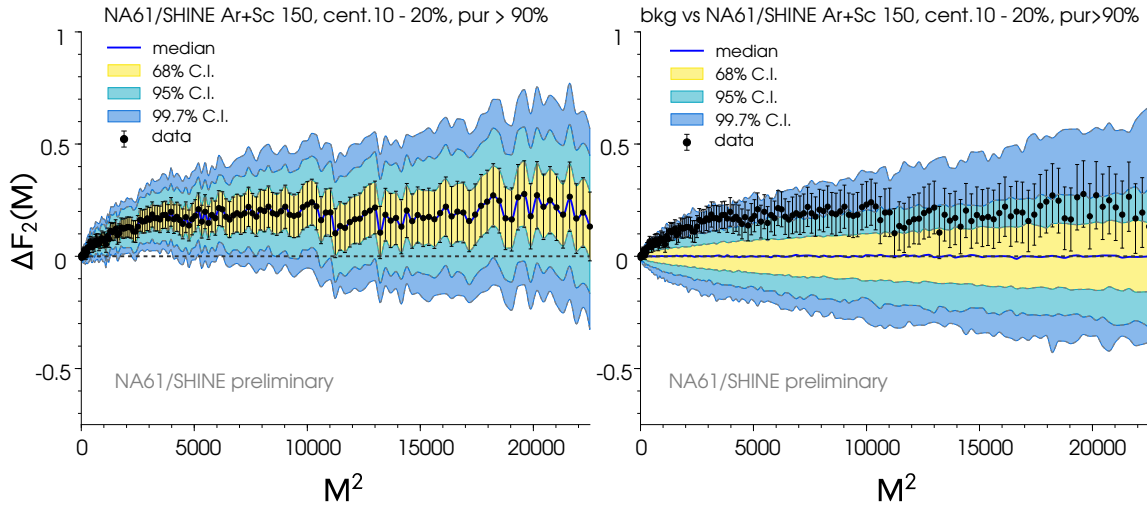


**Figure 12:**  $\Delta F_2(M)$  values distribution for 1000 bootstrap samples of NA61/SHINE Ar+Sc 10-20% most central collisions at 150A GeV/c (left), and for 400 independent samples of random background protons (right). Black points with error bars correspond to the NA61/SHINE Ar+Sc experimental SSFMs, and are shown for comparison with the random background [17].



## 6. Concluding remarks

We have presented a review of the current status of experimentally-oriented intermittency analysis, focusing on proton intermittency. Intermittency analysis of proton density is a promising strategy for detecting the Critical Point of strongly interacting matter. However, it poses certain challenges in the context of an actual heavy-ion collision experiment, which is always constrained in terms of available event statistics, particle multiplicity, and proton identification.

New techniques have been developed, and are constantly being perfected, to allow us to better determine  $\Delta F_2(M)$  and  $\phi_2$  uncertainties. Among these are SSFM and intermittency index error estimation through the statistical bootstrap, as well as AMIAS-assisted weighting of Monte Carlo models used for the evaluation of the possible critical exponents and critical component compatible with what we see in experimental data. Detailed exploration of refined models with critical and non-critical components is certainly needed, in order to assess experimental data. Finally, analysis of different NA61/SHINE systems and collision energies (Pb+Pb, Xe+La) is ongoing, and will hopefully lead to a better mapping of the QCD critical point region, and eventually to the detection of the location of the critical point.

## References

- [1] NA49 collaboration, *Search for the QCD critical point in nuclear collisions at 158A GeV at the CERN Super Proton Synchrotron (SPS)*, *Phys. Rev. C* **81** (2010) 064907.
- [2] NA49 collaboration, *Critical fluctuations of the proton density in A+A collisions at 158A GeV*, *Eur. Phys. J. C* **75** (2015) 587 [1208.5292].
- [3] N.G. Antoniou et al., *Decoding the QCD critical behaviour in A + A collisions*, *Nucl. Phys. A* **1003** (2020) 122018 [2004.12133].
- [4] Y. Hatta and M.A. Stephanov, *Proton number fluctuation as a signal of the QCD critical endpoint*, *Phys. Rev. Lett.* **91** (2003) 102003 [hep-ph/0302002].
- [5] T. Vicsek, *Fractal Growth Phenomena*, World Scientific (1989).
- [6] N.G. Antoniou, Y.F. Contoyiannis, F.K. Diakonou, A.I. Karanikas and C.N. Ktorides, *Pion production from a critical QCD phase*, *Nucl. Phys. A* **693** (2001) 799 [hep-ph/0012164].
- [7] N.G. Antoniou, Y.F. Contoyiannis, F.K. Diakonou and G. Mavromanolakis, *Critical QCD in nuclear collisions*, *Nucl. Phys. A* **761** (2005) 149 [hep-ph/0505185].
- [8] N.G. Antoniou, F.K. Diakonou, A.S. Kapoyannis and K.S. Kousouris, *Critical opalescence in baryonic QCD matter*, *Phys. Rev. Lett.* **97** (2006) 032002 [hep-ph/0602051].
- [9] A. Bialas and R.B. Peschanski, *Moments of Rapidity Distributions as a Measure of Short Range Fluctuations in High-Energy Collisions*, *Nucl. Phys. B* **273** (1986) 703.
- [10] A. Bialas and R.B. Peschanski, *Intermittency in Multiparticle Production at High-Energy*, *Nucl. Phys. B* **308** (1988) 857.

- [11] A. Bialas and R.C. Hwa, *Intermittency parameters as a possible signal for quark - gluon plasma formation*, *Phys. Lett. B* **253** (1991) 436.
- [12] W.J. Metzger, “Estimating the uncertainties of factorial moments.” HEN-455 (unpublished), (2004).
- [13] B. Efron, *Bootstrap Methods: Another Look at the Jackknife*, *The Annals of Statistics* **7** (1979) 1 .
- [14] NA49 collaboration, *The NA49 large acceptance hadron detector*, *Nucl. Instrum. Meth. A* **430** (1999) 210.
- [15] NA61 collaboration, *NA61/SHINE facility at the CERN SPS: beams and detector system*, *JINST* **9** (2014) P06005 [1401.4699].
- [16] NA61/SHINE collaboration, *Search for the critical point of strongly interacting matter through power-law fluctuations of the proton density in NA61/SHINE*, *PoS CPOD2017* (2018) 054.
- [17] NA61/SHINE collaboration, *Searching for the Critical Point of Strongly Interacting Matter in Nucleus–Nucleus Collisions at CERN SPS*, *Acta Phys. Polon. Supp.* **13** (2020) 637 [2002.06636].
- [18] NA61/SHINE collaboration, *Recent results from proton intermittency analysis in nucleus-nucleus collisions from NA61/SHINE at CERN SPS*, *PoS CORFU2018* (2019) 154.
- [19] B. Wosiek, *Intermittency analysis of correlated data*, *Acta Phys. Polon. B* **21** (1990) 1021.
- [20] C. Michael, *Fitting correlated data*, *Phys. Rev. D* **49** (1994) 2616 [hep-lat/9310026].
- [21] E. Stiliaris and C.N. Papanicolas, *Multipole extraction: A Novel, model independent method*, *AIP Conf. Proc.* **904** (2007) 257 [nucl-ex/0703031].
- [22] C.N. Papanicolas and E. Stiliaris, *A novel method of data analysis for hadronic physics*, *arXiv* 1205.6505 (2012) [1205.6505].